

Article

Spin Interference Effects in a Ring with Rashba Spin-Orbit Interaction Subject to Strong Light–Matter Coupling in Magnetic Field

Michal Pudlak ¹  and R. Nazmitdinov ^{2,3,*} ¹ Institute of Experimental Physics, Slovak Academy of Sciences, 040 01 Kosice, Slovakia; pudlak@saske.sk² Bogoliubov Laboratory of Theoretical Physics, Joint Institute for Nuclear Research, 141980 Dubna, Moscow Region, Russia³ Faculty of Natural and Engineering Science, Dubna State University, 141982 Dubna, Russia

* Correspondence: rashid@theor.jinr.ru

Abstract: Electron transport through a one-dimensional quantum ring, subjected to Rashba spin–orbit interaction and connected with two external leads, is studied in the presence of external fields. They include the optical radiation, produced by an off-resonant high-frequency electric field, and a perpendicular magnetic field. By means of the Floquet theory of periodically driven quantum systems the interference effects under these fields are described in detail. It is found analytically the specific conditions to reach the spin-filtering effect, caused by the interplay of the external fields and Rashba spin-orbit interaction.

Keywords: Rashba spin–orbit interaction; semiconductor quantum ring; Floquet theory; light–matter coupling; magnetic field



Citation: Pudlak, M.; Nazmitdinov, R. Spin Interference Effects in a Ring with Rashba Spin-Orbit Interaction Subject to Strong Light–Matter Coupling in Magnetic Field. *Symmetry* **2022**, *14*, 1194. <https://doi.org/10.3390/sym14061194>

Academic Editor: Charalampos Moustakidis

Received: 24 May 2022

Accepted: 6 June 2022

Published: 9 June 2022

Publisher’s Note: MDPI stays neutral with regard to jurisdictional claims in published maps and institutional affiliations.



Copyright: © 2022 by the authors. Licensee MDPI, Basel, Switzerland. This article is an open access article distributed under the terms and conditions of the Creative Commons Attribution (CC BY) license (<https://creativecommons.org/licenses/by/4.0/>).

1. Introduction

Progress in nanotechnology raised a tremendous activity in the field of quantum electronics. In particular, a special attention is paid to the possibility to use spin–orbit interaction (SOI) for the design of nanoelectronic devices, based on control of electron spin without application of the magnetic field. In semiconductors there are two mechanisms of SOI: the Dresselhaus SOI [1], caused by the inversion asymmetry of the crystal lattice; the Rashba SOI [2], produced by the inversion asymmetry of a heterostructure. It is important to note that the strength of the Dresselhaus SOI is determined exclusively by the material, while the strength of the Rashba SOI can be by altered externally, for example, by means of a gate voltage. Therefore, the vast majority of literature, devoted to spin-dependent transport in nanostructures, is focused on materials with spin–orbit interaction of Rashba type (e.g., Refs. [3,4]).

It was recently proposed to use a strong off-resonant optical field to manipulate spin–orbit coupling [5]. In this case there is no real absorption of the wave. This is so-called regime of strong light–matter interaction, when quantum nature of light can drastically modify the properties of the matter itself. In fact, recent progress in laser physics provides the possibility to use optical high-frequency fields to control various atomic and condensed-matter structures, based on the Floquet theory of periodically driven quantum systems (e.g., Refs. [6–8]). The concept of radiation-dressed states in atom [9] is the fundamental background for this consideration. In this case, the hybrid electron-field object (dressed electron) represents an elementary quasiparticle, which physical properties can differ sufficiently from the “bare” electron.

Thanks to new generation of high-efficient lasers, this phenomenon may render possible its wide application in semiconductor physics. In particular, physical properties of dressed electrons have been studied in quantum wells [10], quantum rings [11,12], and

topological insulators [13,14]. Evidently, this phenomenon becomes quite attractive for spintronics as well, since the spin of individual carriers can be controlled by optical means with or without application of the magnetic field, indeed. From this point of view semiconductor quantum rings with the Rashba SOI represent a fertile ground in the regime of strong light–matter coupling for applied physics, as well as for study of effects of different geometric phases [15]. The control of electron spin by means of the optical method and by a weak external magnetic field, and its consequences for transport properties in the above system have been escaped in previous studies (see, e.g., Refs. [3,16–20] and references therein). The main goal of this paper is to fill this gap in the case of the ring with the Rashba SOI for dressed electrons in magnetic field.

2. Model

2.1. The Hamiltonian

To analyse the regime of strong light–matter interaction, we consider the two-dimensional (2D) Hamiltonian describing ballistic electrons of charge $-e$ ($e > 0$) and the effective mass m , in the presence of the Rashba SOI, a magnetic field and a high-frequency electric field:

$$\hat{H} = \frac{1}{2m}\mathbf{\Pi}^2 + \alpha(\boldsymbol{\sigma} \times \mathbf{\Pi})_z + g\mu\boldsymbol{\sigma}\mathbf{B} + V(\mathbf{r}). \tag{1}$$

Here $\boldsymbol{\sigma}$ is the vector of the Pauli spin matrices, $\mathbf{\Pi} = \mathbf{p} + e\mathbf{A}$, α is the strength of the Rashba SOI. The vector potential of a linear polarised electromagnetic wave $\mathbf{A} = ([E_0/\omega] \cos(\omega t) - By/2, Bx/2, 0)$ includes the magnetic field \mathbf{B} , pointing in the z direction (perpendicular to the plane). The electric field is characterised by the amplitude E_0 and by the wave frequency ω . We consider a narrow ring, characterised by a steep confining potential $V(\mathbf{r})$. If the field is time-independent and $E_0 = 0$, in such a ring geometry the electron energy spectrum is determined by the 1D Hamiltonian in polar coordinates (see also [17,21]):

$$\hat{H}_R^{(0)} = \frac{\hbar^2}{2mR^2} \left(-i\frac{\partial}{\partial\varphi} + \frac{\Phi}{\Phi_0} \right)^2 + \frac{\hbar\omega_B}{2}\sigma_z + \hbar\omega_R\sigma_x(\varphi) \left(-i\frac{\partial}{\partial\varphi} + \frac{\Phi}{\Phi_0} \right) - i\frac{\hbar\omega_R}{2}\sigma_y(\varphi). \tag{2}$$

Here, $\omega_B = 2\mu B/\hbar$, $\omega_R = \alpha/R$, $\sigma_x(\varphi) = \cos\varphi\sigma_x + \sin\varphi\sigma_y$, $\sigma_y(\varphi) = \cos\varphi\sigma_y - \sin\varphi\sigma_x$, φ is the polar angle of the electron on the ring, $\Phi = \pi BR^2$ is the magnetic flux through the ring, and the magnetic flux quantum $\Phi_0 = h/e$. Once we add a time-dependent electric field the Hamiltonian of an irradiated ring takes the following form

$$\hat{H}_{1D} = \hat{H}_R + \left[\sum_{n=1}^2 \hat{V}_n e^{in\omega t} + H.c \right], \tag{3}$$

where the stationary term is complemented by a field-induced constant energy shift

$$\hat{H}_R = \hat{H}_R^{(0)} + E_{shift}^{(0)}, \quad E_{shift}^{(0)} = \frac{e^2 E_0^2}{4m\omega^2}. \tag{4}$$

The periodic term consists of two harmonics, raised by the irradiation,

$$\hat{V}_1 = -\frac{eE_0}{2mR\omega} \left(\sin\varphi \hat{l}_{z,\Phi} - i\hbar \frac{\cos\varphi}{2} \right] - \frac{\alpha e E_0}{2\omega} \sigma_y, \tag{5}$$

$$\hat{V}_2 = \frac{e^2 E_0^2}{8m\omega^2}, \tag{6}$$

and we introduce the notation $\hat{l}_{z,\Phi} = -i\hbar\partial_\varphi + \hbar\Phi/\Phi_0$.

In the following we employ the high-frequency approximation for a periodically driven quantum system (for a review see, e.g., Ref. [22]). Such the approach provides a systematic high-frequency expansion for the effective Hamiltonian. In our analysis, we

consider only the leading terms in the high-frequency limit. As a result, we can reduce the time-dependent Hamiltonian (3) to the effective time-independent one (see also [19]):

$$\hat{\mathcal{H}} = \hat{H}_R + \sum_{n=1}^2 \frac{[\hat{V}_n, \hat{V}_n^\dagger]}{n\hbar\omega} + \sum_{n=1}^2 \frac{[\hat{V}_n, \hat{H}_R], \hat{V}_n^\dagger + H.c.}{2(n\hbar\omega)^2} = \hat{\mathcal{H}}_0 + \hat{V}, \tag{7}$$

where

$$\begin{aligned} \hat{\mathcal{H}}_0 &= \frac{\hat{l}_{z,\Phi}^2}{2m^*R^2} + \omega_R \left[\sigma_x(\varphi)\hat{l}_{z,\Phi} - i\hbar \frac{\sigma_y(\varphi)}{2} \right] - \left(\frac{eE_0\alpha}{R\omega^2} \right)^2 \frac{\hat{l}_{z,\Phi}}{m\hbar} \sigma_z \\ &+ \frac{\hbar\omega_B}{2} \sigma_z + E_{shift}^{(0)} + E_{shift}^{(1)}, \quad E_{shift}^{(1)} = \frac{1}{2m} \left(\frac{\hbar eE_0}{4mR^2\omega^2} \right)^2 \end{aligned} \tag{8}$$

$$\hat{V} = \frac{\hbar^2}{2mR^2} \left[\hat{V}_a + \hat{V}_b + \left(\frac{\gamma_1 \hat{l}_{z,\Phi}}{2\hbar} \right)^2 \cos 2\varphi \right], \tag{9}$$

$$\hat{V}_a = \left[\frac{3}{16} \gamma_1^2 \cos 2\varphi - i\gamma_1^2 \gamma_2 \left(\gamma_2^2 - \frac{1}{4} \right) \sigma_x \sin \varphi \right], \tag{10}$$

$$\hat{V}_b = \left[\frac{i}{2} \gamma_1^2 \sin 2\varphi - 2\gamma_1^2 \gamma_2 \left(\gamma_2^2 - \frac{1}{4} \right) \sigma_x \cos \varphi \right] \frac{\hat{l}_{z,\Phi}}{\hbar}. \tag{11}$$

Here, we introduce the following notations:

$$\gamma_1 = eE_0/(mR\omega^2), \quad \gamma_2 = mR\alpha/\hbar, \quad m^* = \frac{m}{1 + 3(\gamma_1/2)^2}. \tag{12}$$

The irradiation leads to the mass renormalization, i.e., $m \rightarrow m^*$. It yields as well the energy shift to the zero energy $\Delta E = E_{shift}^{(0)} + E_{shift}^{(1)}$, and introduces the coupling between the strength of the Rashba SOI and the ring radius by means of the parameter γ_2 .

2.2. The Eigenvalue Problem

The Hamiltonian (7) possess the azimuthal symmetry. The operator $\hat{J}_z = I \otimes (-i\hbar\partial_\varphi) + \hbar\sigma_z/2$, defined in the laboratory frame, is an integral of motion $[\mathcal{H}, \hat{J}_z] = 0$. Let us analyse, first, the eigenvalue problem for the Hamiltonian (8). It is convenient to transform this Hamiltonian in the rotating frame by means of the unitary transformation $R = \exp[i(\sigma_z/2)\varphi]$. As a result, we obtain

$$\hat{H} = R\mathcal{H}_0R^\dagger = \frac{\hat{X}_{z,\Phi}^2}{2m^*R^2} + \frac{\alpha}{R} \left[\sigma_x \hat{X}_{z,\Phi} - i\hbar \frac{\sigma_y}{2} \right] - \left(\frac{eE_0\alpha}{R\omega^2} \right)^2 \frac{\hat{X}_{z,\Phi}}{m\hbar} \sigma_z + \frac{\hbar\omega_B}{2} \sigma_z + \Delta E. \tag{13}$$

$$\hat{X}_{z,\Phi} = -i\hbar\partial_\varphi + \hbar\Phi/\Phi_0 - \hbar \frac{\sigma_z}{2}. \tag{14}$$

In the rotating frame the operator \hat{J}_z takes the following form

$$\hat{J}_z = R\hat{J}_zR^\dagger = I \otimes (-i\hbar\partial_\varphi). \tag{15}$$

Consequently, we search the eigenfunctions of the Hamiltonian (13) in a general form

$$\Phi_j^s(\varphi) = e^{ij\varphi} \chi_j^s, \quad \chi_j^s = \begin{pmatrix} \chi_1^s \\ \chi_2^s \end{pmatrix}. \tag{16}$$

Evidently, the eigenvalues of the operator \hat{J} are expected to be half-integers in the laboratory frame, that should be hold in the rotating frame as well ($RR^{-1} = 1$)

$$\hat{J}_z \Phi_j^s(\varphi) = \hbar j \Phi_j^s(\varphi), \quad j = \lambda n + 1/2, \quad n = 1, 2, 3, \dots \tag{17}$$

Here, the orbital quantum number n corresponds to the electron rotation either in the counterclockwise direction $\lambda = +1$, or in the clockwise one $\lambda = -1$. The solution of the Schrödinger equation by means of the probe functions (16) yields the eigenenergies

$$E_j^s = \hbar\omega_0 \left[\left(j + \frac{\Phi}{\Phi_0} \right)^2 + \frac{1}{4} + s \sqrt{\Omega^2 + \left(\frac{m^*}{m} \right)^2 Q_R^2 \left(j + \frac{\Phi}{\Phi_0} \right)^2} \right] + \Delta E; \quad s = \pm 1, \quad (18)$$

where

$$\Omega = \frac{\omega_B}{2\omega_0} - \left[1 + 2Q_E^2 \frac{m^*}{m} \right] \left(j + \frac{\Phi}{\Phi_0} \right). \quad (19)$$

Here, we introduce the following definitions: $\omega_0 = \hbar/(2m^*R^2)$, $Q_E = eE_0\alpha/(\hbar\omega^2)$, and $Q_R = 2m\alpha R/\hbar$. For the eigenfunctions we obtain two sets

$$\chi_j^{(s=1)} = \begin{pmatrix} \sin \frac{\gamma}{2} \\ \cos \frac{\gamma}{2} \end{pmatrix}, \quad \chi_j^{(s=-1)} = \begin{pmatrix} \cos \frac{\gamma}{2} \\ -\sin \frac{\gamma}{2} \end{pmatrix}, \quad (20)$$

where

$$\tan \gamma = \frac{\alpha\hbar/R \left(j + \frac{\Phi}{\Phi_0} \right)}{\Omega} = \frac{Q_R m^*/m}{1 + 2Q_E^2 m^*/m - \omega_B/[2\omega_0(j + \Phi/\Phi_0)]}, \quad (21)$$

γ is the angle between the local spin quantization axis and the z -axis. The high-frequency (dressing) field decreases this angle relative to its value $\tan \gamma = Q_R$, obtained in Ref. [20] without the external electric field ($E_0 = 0$) and Zeeman interaction. Evidently, a proper choice of the Rashba coupling and parameters of the external high-frequency electric field may lead to new features of the considered system (see below).

The eigenstates of the Hamiltonian (8) are defined in the laboratory frame as

$$\Psi_j^s(\varphi) = e^{-i\frac{\sigma_z}{2}\varphi} \Phi_j^s(\varphi) = e^{ij\varphi} e^{-i\frac{\sigma_z}{2}\varphi} \chi_j^s. \quad (22)$$

Before proceeding further, there are a few comments required. The total effective Hamiltonian (7) consists of the discussed Hamiltonian (8) and the term \hat{V} . The terms (9)–(11) are of order $\sim \gamma_1^2$. In the high-frequency approximation, considered in our paper, $\gamma_1 \ll 1$. Consequently, we neglect the contribution of the above terms, and will analyse the transport properties of semiconductor quantum rings with the reduced Hamiltonian (8) (see also the discussion in Ref. [19]). For a typical semiconductor (for example, GaAs) the magnetic orbital effect is much enhanced in comparison with the magnetic spin effect (see, e.g., Ref. [23]). Moreover, we will consider the effect of the weak magnetic field (see below). Consequently, without loss of generality, we can neglect the Zeeman effect in Equations (19) and (21) and obtain

$$E_{\lambda,n}^s = \hbar\omega_0 \left[\left(\lambda n + \frac{1}{2} + \frac{\Phi}{\Phi_0} \right)^2 + \frac{1}{4} + s \left| \lambda n + \frac{1}{2} + \frac{\Phi}{\Phi_0} \right| \times \right. \quad (23)$$

$$\left. \times \sqrt{\left[1 + 2Q_E^2 \frac{m^*}{m} \right]^2 + \left(\frac{m^*}{m} \right)^2 Q_R^2} \right],$$

where the energy shift ΔE is omitted, since it is the same constant for the electron dressed levels. In the case: (i) $E_0 = 0$; (ii) $\mathbf{B} = 0$, the reduced energies Equation (23) are equivalent to the energies obtained in Ref. [17]. These energies are maximised for the up spin states $|\uparrow\rangle$, i.e., for $s = 1$; and the factor Q_R plays the important role in transport properties. The external high-frequency electric field gives rise to the additional factor Q_E . As we will see below, its interplay with the factor Q_R leads to novel phenomena in transport properties of the semiconductor rings.

3. Transport Properties

In this section, we investigate the effect of two factors, Q_R and Q_E , on the conductance and the polarization of the ballistic current in our 1D model. To model realistic transport, it is desirable to take into account the effects of disorder. Since we consider the high-frequency limit (a semiclassical regime), there are different classical paths connecting the entrance and exit attached leads. It seems reasonable to assume that only pairs with the same length could contribute essentially to the conductance. In our consideration we assume a perfect coupling between leads and ring, neglecting the backscattering effects. In other words, in our model the interference effects arising from counterclockwise and clockwise waves.

Thus, the wave function of an incoming electron from the left lead, attached to the ring, is split at the ring entrance into four partial waves. In particular, we consider that electrons with Fermi energy E_F move from the entrance to the exit with four different wave numbers $n \Rightarrow \lambda n_\lambda^s$. In this case the eigenstates (22) can be written as (see also the discussion in Ref. [17])

$$\Psi_{+n}^1(\varphi) = e^{in_+^1\varphi} \begin{pmatrix} \sin \frac{\gamma}{2} \\ \cos \frac{\gamma}{2} e^{i\varphi} \end{pmatrix}, \quad (24)$$

$$\Psi_{+n}^{-1}(\varphi) = e^{in_+^{-1}\varphi} \begin{pmatrix} \cos \frac{\gamma}{2} \\ -\sin \frac{\gamma}{2} e^{i\varphi} \end{pmatrix}, \quad (25)$$

$$\Psi_{-n}^1(\varphi) = e^{-in_-^1\varphi} \begin{pmatrix} \cos \frac{\gamma}{2} \\ -\sin \frac{\gamma}{2} e^{i\varphi} \end{pmatrix}, \quad (26)$$

$$\Psi_{-n}^{-1}(\varphi) = e^{-in_-^{-1}\varphi} \begin{pmatrix} \sin \frac{\gamma}{2} \\ \cos \frac{\gamma}{2} e^{i\varphi} \end{pmatrix}. \quad (27)$$

They meet at the exit (a right attached lead), exactly opposite to the entrance. The wave, propagating clockwise, travels the angle $-\pi$ from the entrance to the exit. The wave, propagating counterclockwise, travels the angle π from the entrance to the exit.

3.1. Conductance

In order to analyse the conductance we use the Landauer–Büttiker formalism. In this case the conductance at zero temperature has the following form (see, e.g., Ref. [24])

$$G = \frac{e^2}{h} \sum_{s,s'} T_{s,s'}. \quad (28)$$

Here, $T_{s,s'} = |t_{s,s'}|^2$ is the quantum probability of transmission between incoming state with spin s' and outgoing state with spin s ; $t_{s,s'}$ is the corresponding transmission amplitude. Using the results from Appendix A, we arrive to the expression

$$G = \frac{e^2}{h} \left[1 + \frac{1}{2} [\cos \pi(n_-^{-1} - n_+^{+1}) + \cos \pi(n_-^{+1} - n_+^{-1})] \right]. \quad (29)$$

The quantities n_λ^s can be obtained from the solution of Equation (18) at the condition $E_{\lambda,n}^s = E_F$ for different spin orientation $s = \pm 1$.

$$n_-^{-1} - n_+^{+1} = 1 + 2 \frac{\Phi}{\Phi_0} + \sqrt{\left[1 + 2Q_E^2 \frac{m^*}{m} \right]^2 + \left(\frac{m^*}{m} \right)^2 Q_R^2}, \quad (30)$$

$$n_-^{+1} - n_+^{-1} = 1 + 2 \frac{\Phi}{\Phi_0} - \sqrt{\left[1 + 2Q_E^2 \frac{m^*}{m} \right]^2 + \left(\frac{m^*}{m} \right)^2 Q_R^2}. \quad (31)$$

Taking into account Equations (30) and (31), we arrive to the final expression for the conductance

$$G = \frac{e^2}{h} \left[1 - \cos\left(2\pi \frac{\Phi}{\Phi_0}\right) \cos \pi \sqrt{\left[1 + 2Q_E^2 \frac{m^*}{m}\right]^2 + \left(\frac{m^*}{m}\right)^2 Q_R^2} \right]. \tag{32}$$

Now we are ready to trace the conductance behaviour as a function of the following variables: (i) the strength of the Rashba interaction α ; (ii) the electric field E_0 ; and (iii) the magnetic field. As a typical example, we consider InGaAs-based quantum rings with the following parameters: the effective mass $m = 0.045m_e$, radius $R \approx 200$ nm, and the strength of the Rashba SOI $\alpha \approx 10^4$ m/s. The effective mass and the radius determine the energy scale $\hbar\omega_0 \equiv \hbar^2/(2mR^2) \approx 2.16 \times 10^{-5}$ eV at $m^* = m$. Assuming the maximal flux $\Phi = 0.5\Phi_0$ through the ring in our consideration, we obtain

$$\mu B = \frac{e\hbar}{2m_e} \times \frac{\hbar}{e} \frac{1}{R^2} \ll \hbar\omega_0. \tag{33}$$

Our approximation (neglecting the Zeeman term) is quite satisfactory, indeed.

At zero magnetic and electric fields the conductance is modulated by the strength Q_R alone [17]. Taking into account that the amplitude

$$E_0 = \sqrt{\frac{2I}{\epsilon_0 c}}, \tag{34}$$

where I is the irradiance intensity, ϵ_0 is the vacuum permittivity, we can enrich the interference of the conductance from the destructive to constructive and vice versa by altering the intensity at a fixed value of the Rashba SOI α (see Figure 1). Once we switch on the magnetic field, the conductance modulations are reversed (see Figure 2). Moreover, the oscillations are removed with a proper choice of of the Rashba SOI strength.

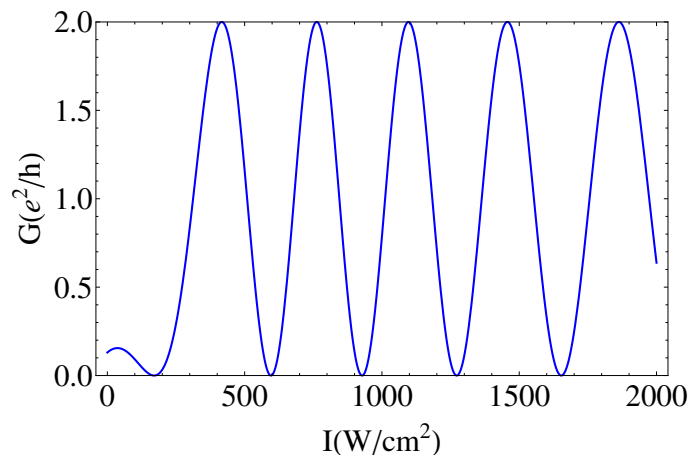


Figure 1. Conductance versus irradiation intensity I . Electron effective mass $m = 0.045m_e$, the Rashba coupling constant $\alpha = 5 \times 10^4$ ms⁻¹, and the ring radius is $R = 200$ nm. The dressing field has the frequency $\omega = 1.6 \times 10^{12}$ s⁻¹, the magnetic flux $\Phi = 0$.

Thus, the magnetic field provides the additional key element of possible ring-shaped spintronic devices operated by light.

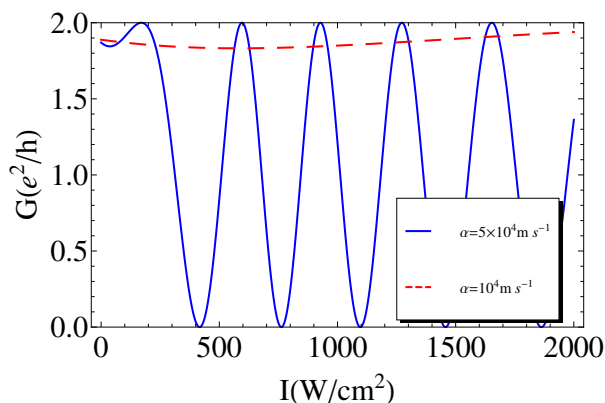


Figure 2. Conductance versus irradiation intensity I for different Rashba coupling constant α . Electron effective mass $m = 0.045m_e$ and the ring radius is $R = 200$ nm. The dressing field has the frequency $\omega = 1.6 \times 10^{12} \text{ s}^{-1}$, the magnetic flux $\Phi = 0.5\Phi_0$.

To get deeper inside let us consider the minimum of the conductance at $m^* = m$. At zero magnetic field, we have the condition

$$\cos \pi \sqrt{\left[1 + 2Q_E^2 \frac{m^*}{m}\right]^2 + \left(\frac{m^*}{m}\right)^2 Q_R^2} = 1, \tag{35}$$

which is subject to the equation

$$\sqrt{\left[1 + 2Q_E^2\right]^2 + Q_R^2} = 2n, \quad n = 1, 2, \dots \tag{36}$$

By introducing the variables

$$\sin \gamma = \frac{Q_R}{2n}, \quad \cos \gamma = \frac{1 + 2Q_E^2}{2n}, \tag{37}$$

we arrive to Equation (21) at $\omega_B = 0$. Thus, the single-valuedness of the eigenfunctions (20) determines the character of the conduction modulations (35).

3.2. Spin-Filtering Effect

The question we address in this section is could we control the polarization of the electron beam by means of our quantum ring with the aid of the intensity of the external electric field and with the strength of the vertical magnetic field?

The spin polarization P , determined as

$$P = \frac{T_{\uparrow\uparrow} + T_{\downarrow\downarrow} - T_{\downarrow\uparrow} - T_{\uparrow\downarrow}}{T_{\uparrow\uparrow} + T_{\downarrow\downarrow} + T_{\downarrow\uparrow} + T_{\uparrow\downarrow}}, \tag{38}$$

in virtue of the results for transmission probabilities $T_{\sigma\sigma'}$ (see Appendix A), yields

$$P = \cos 2\gamma \frac{\sin\left(2\pi \frac{\Phi}{\Phi_0}\right) \sin \pi \sqrt{\left[1 + 2Q_E^2 \frac{m^*}{m}\right]^2 + \left(\frac{m^*}{m}\right)^2 Q_R^2}}{1 - \cos\left(2\pi \frac{\Phi}{\Phi_0}\right) \cos \pi \sqrt{\left[1 + 2Q_E^2 \frac{m^*}{m}\right]^2 + \left(\frac{m^*}{m}\right)^2 Q_R^2}}. \tag{39}$$

From Equation (39) it follows that the presence of the magnetic field is the basic condition for the polarization process, since $P = 0$ at $\Phi = n\Phi_0/2, n = 0, 1, 2, \dots$. On the

other hand, once the magnetic field takes, for example, the value $\Phi/\Phi_0 = 1/4$, we can require that

$$\sin \pi \sqrt{\left[1 + 2Q_E^2 \frac{m^*}{m}\right]^2 + \left(\frac{m^*}{m}\right)^2} Q_R^2 = 1. \tag{40}$$

Without loss of generality we consider the case $m^* = m$ and obtain

$$\sin \gamma = \frac{Q_R}{k}, \quad \cos \gamma = \frac{(1 + 2Q_E^2)}{k}, \quad k = 2n + 1/2, \quad n = 0, 1, 2, \dots \tag{41}$$

In this case the polarization is defined as

$$P = \cos 2\gamma = [(1 + 2Q_E^2)^2 - Q_R^2]/k^2. \tag{42}$$

At a fixed value of the strength of the Rashba SOI, we can define the value of the intensity of the electric field that could provide the maximal polarization $P = 1$ (see Figure 3).

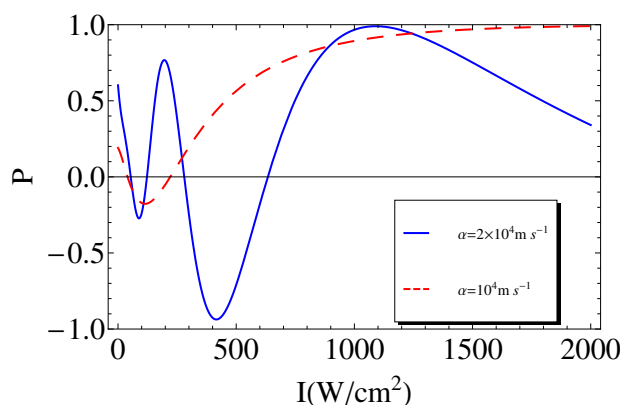


Figure 3. Spin polarization P versus the irradiation intensity I . The calculations are performed at the magnetic flux $\Phi = 0.25\Phi_0$; the dressing field frequency is $\omega = 0.8 \times 10^{12} \text{ s}^{-1}$. The solid (blue) line corresponds to the strength $\alpha = 2 \times 10^4 \text{ m/s}$, while the dashed (red) line corresponds to $\alpha = 10^4 \text{ m/s}$.

For example, taking into account the definition of $Q_E = eE_0\alpha / (\hbar\omega^2)$ and the intensity (34), we have at $k = 1/2$

$$2Q_E^2 = \sqrt{Q_R^2 + \frac{1}{4}} - 1 = \frac{4I}{\epsilon_0 c} \left(\frac{\hbar\omega^2}{e\alpha}\right)^2. \tag{43}$$

From Equation (43) it follows evidently that $Q_E > 0$ if the following relation takes place (taking into account the definition $Q_R = (2mR/\hbar)\alpha$)

$$\alpha > \frac{\sqrt{3}}{2} R\omega_0. \tag{44}$$

Once this condition is fulfilled, the minimal value of the intensity is

$$I = \frac{\epsilon_0 c}{4} \left(\frac{\hbar\omega^2}{e\alpha}\right)^{-2} \left[\sqrt{Q_R^2 + \frac{1}{4}} - 1\right], \tag{45}$$

that allows to observe the spin-filtering effect in our system. Altering the value of the magnetic field, we can decrease, as well, the dynamic threshold intensity field at a fixed value of the strength of the Rashba SOI (see Figure 4).

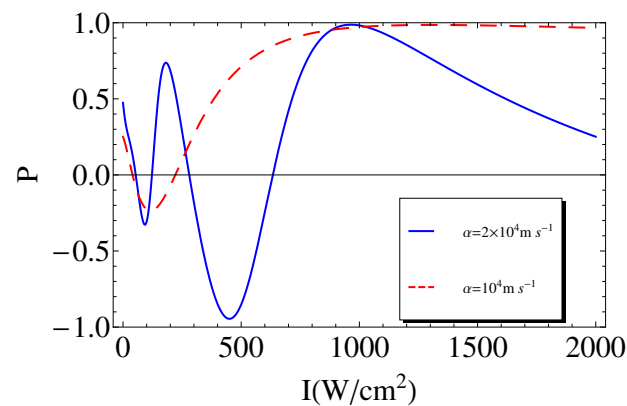


Figure 4. Similar to Figure 3 at the magnetic flux $\Phi = 0.2\Phi_0$.

4. Conclusions

The effect of a high-frequency optical field and an external magnetic field on quantum transport through the one-dimensional quantum ring subject to Rashba SOI is manifested in a rich variety of phenomena. To carry on our analysis of the external fields, we employed the Floquet theory of periodically driven quantum system. In our consideration we assumed a perfect coupling between leads and ring, neglecting the backscattering effects. In this limit, several mechanisms, responsible for quantum interference effects have been proposed. In particular, it shown that the conductance oscillations, produced by the ring irradiated by the dressing field, can be reversed by the application of the weak magnetic field (compare Figures 1 and 2). In other words, our system behaves like a diode, operating at a certain intensity of the dressing field, that allows the current flow only at a certain value of the external magnetic field. Finally, we formulated analytically the requirements to reach the spin-filtering effects under the external fields (see Section 3.2). Our findings may provide new capabilities for spintronics devices, exploiting the combined effect of optical and magnetic fields.

Author Contributions: All authors contributed equally to this work. All authors have read and agreed to the published version of the manuscript.

Funding: This research received no external funding.

Institutional Review Board Statement: Not applicable.

Informed Consent Statement: Not applicable.

Data Availability Statement: Not applicable.

Conflicts of Interest: The authors declare no conflict of interest.

Abbreviations

The following abbreviations are used in this manuscript:

MDPI Multidisciplinary Digital Publishing Institute
DOAJ Directory of open access journals
TLA Three letter acronym

Appendix A. Transmission Probabilities

Let us consider the case of the incoming electron with spin \uparrow ($s = +1$) [see Equation (20)] entering the ring at $\varphi = 0$

$$|\uparrow\rangle = \begin{pmatrix} \sin \frac{\gamma}{2} \\ \cos \frac{\gamma}{2} \end{pmatrix}. \quad (\text{A1})$$

Evidently, states of a particular spin split equally into the clockwise path ($\lambda = -1$) and the counterclockwise path ($\lambda = 1$) in the ring

$$|\Psi(\uparrow, \varphi)\rangle = \frac{1}{2} \exp[in_+^{+1}\varphi] \begin{pmatrix} \sin \frac{\gamma}{2} \\ \cos \frac{\gamma}{2} e^{i\varphi} \end{pmatrix} + \frac{1}{2} \exp[-in_-^{-1}\varphi] \begin{pmatrix} \sin \frac{\gamma}{2} \\ \cos \frac{\gamma}{2} e^{i\varphi} \end{pmatrix} \quad (A2)$$

Additionally, in particular, we have at the exit of the ring

$$|\Psi(\uparrow, \pi)\rangle = \frac{1}{2} \exp[in_+^{+1}\pi] \begin{pmatrix} \sin \frac{\gamma}{2} \\ \cos \frac{\gamma}{2} e^{i\pi} \end{pmatrix} + \frac{1}{2} \exp[-in_-^{-1}(-\pi)] \begin{pmatrix} \sin \frac{\gamma}{2} \\ \cos \frac{\gamma}{2} e^{-i\pi} \end{pmatrix} \quad (A3)$$

Consequently, the probability amplitude without the spin flip for the incoming electron with spin \uparrow is

$$t_{\uparrow\uparrow} = \langle \uparrow | \Psi(\uparrow, \pi) \rangle, \quad (A4)$$

which determines the corresponding transmission probability as

$$T_{\uparrow\uparrow} = |t_{\uparrow\uparrow}|^2 = \frac{1}{2} \cos^2 \gamma [1 + \cos \pi(n_-^{-1} - n_+^{+1})]. \quad (A5)$$

The amplitude of probability that the incoming electron with spin \uparrow is outgoing with the spin \downarrow [see Equation (20)] is

$$t_{\downarrow\uparrow} = \langle \downarrow | \Psi(\uparrow, \pi) \rangle, \quad |\downarrow\rangle = \begin{pmatrix} \cos \frac{\gamma}{2} \\ -\sin \frac{\gamma}{2} \end{pmatrix}, \quad (A6)$$

which yields the following result

$$T_{\downarrow\uparrow} = |t_{\downarrow\uparrow}|^2 = \frac{1}{2} \sin^2 \gamma [1 + \cos \pi(n_-^{-1} - n_+^{+1})]. \quad (A7)$$

Let us consider the case of the incoming electron with spin \downarrow ($s = -1$) [see Equation (20)] entering the ring at $\varphi = 0$. In this case electron traverses the ring, and its wave function [see Equations (25) and (26)] is

$$|\Psi(\downarrow, \varphi)\rangle = \frac{1}{2} \exp[in_+^{-1}\varphi] \begin{pmatrix} \cos \frac{\gamma}{2} \\ -\sin \frac{\gamma}{2} e^{i\varphi} \end{pmatrix} + \frac{1}{2} \exp[-in_-^{+1}\varphi] \begin{pmatrix} \cos \frac{\gamma}{2} \\ -\sin \frac{\gamma}{2} e^{i\varphi} \end{pmatrix}. \quad (A8)$$

It takes the following form at the exit of the ring

$$|\Psi(\downarrow, \varphi)\rangle = \frac{1}{2} \exp[in_+^{-1}\pi] \begin{pmatrix} \cos \frac{\gamma}{2} \\ -\sin \frac{\gamma}{2} e^{i\pi} \end{pmatrix} + \frac{1}{2} \exp[-in_-^{+1}(-\pi)] \begin{pmatrix} \cos \frac{\gamma}{2} \\ -\sin \frac{\gamma}{2} e^{i(-\pi)} \end{pmatrix}. \quad (A9)$$

For the amplitude of probability that the incoming electron with spin \downarrow is outgoing with spin \downarrow we have

$$t_{\downarrow\downarrow} = \langle \downarrow | \Psi(\downarrow, \pi) \rangle. \quad (A10)$$

Consequently, the corresponding transmission probability is

$$T_{\downarrow\downarrow} = |t_{\downarrow\downarrow}|^2 = \frac{1}{2} \cos^2 \gamma [1 + \cos \pi(n_-^{+1} - n_+^{-1})]. \quad (A11)$$

The amplitude of probability that the incoming electron with spin \downarrow is outgoing with spin \uparrow is

$$t_{\uparrow\downarrow} = \langle \uparrow | \Psi(\downarrow, \pi) \rangle. \quad (A12)$$

It results in the following transmission probability

$$T_{\uparrow\downarrow} = |t_{\uparrow\downarrow}|^2 = \frac{1}{2} \sin^2 \gamma [1 + \cos \pi(n_-^{+1} - n_+^{-1})]. \quad (A13)$$

References

1. Dresselhaus, G. Spin-orbit coupling effects in zinc blende structures. *Phys. Rev.* **1955**, *100*, 580. [[CrossRef](#)]
2. Bychkov, Y.A.; Rashba, E.I. Properties of a 2D electron gas with lifted spectral degeneracy. *JETP Lett.* **1984**, *39*, 78.
3. Bercioux, D.; Lucignano, P. Quantum transport in Rashba spin-orbit materials: A review. *Rep. Prog. Phys.* **2015**, *78*, 106001. [[CrossRef](#)] [[PubMed](#)]
4. Pichugin, K.; Puente, A.; Nazmitdinov, R. Kramers degeneracy and spin inversion in a lateral quantum dot. *Symmetry* **2020**, *12*, 2043. [[CrossRef](#)]
5. Sheremet, A.S.; Kibis, O.V.; Kavokin, A.V.; Shelykh, I.A. Datta-and-Das spin transistor controlled by a high-frequency electromagnetic field. *Phys. Rev. B* **2016**, *93*, 165307. [[CrossRef](#)]
6. Goldman, N.; Dalibard, J. Periodically Driven Quantum Systems: Effective Hamiltonians and Engineered Gauge Fields. *Phys. Rev. X* **2014**, *4*, 031027. [[CrossRef](#)]
7. Holthaus, M. Floquet engineering with quasienergy bands of periodically driven optical lattices. *J. Phys. B* **2016**, *49*, 013001. [[CrossRef](#)]
8. Meinert, F.; Mark, M.J.; Lauber, K.; Daley, A.J.; Nägerl, H.-C. Floquet Engineering of Correlated Tunneling in the Bose-Hubbard Model with Ultracold Atoms. *Phys. Rev. Lett.* **2016**, *116*, 205301. [[CrossRef](#)]
9. Cohen-Tannoudji, C.; Dupont-Roc, J.; Grynberg, G. *Atom-Photon Interactions: Basic Processes and Applications*; Wiley-VCH: Hoboken, NJ, USA, 2004.
10. Teich, M.; Wagner, M.; Schneider, H.; Helm, M. Semiconductor quantum well excitons in strong, narrowband terahertz fields. *New J. Phys.* **2013**, *15*, 065007. [[CrossRef](#)]
11. Joibari, F.K.; Blanter, Y.M.; Bauer, G.E.W. Light-induced spin polarizations in quantum rings. *Phys. Rev. B* **2014**, *90*, 155301. [[CrossRef](#)]
12. Koshelev, K.L.; Kachorovskii, V.Y.; Titov, M. Resonant inverse Faraday effect in nanorings. *Phys. Rev. B* **2015**, *92*, 235426. [[CrossRef](#)]
13. Foa Torres, L.E.F.; Perez-Piskunow, P.M.; Balseiro, C.A.; Usaj, G. Multiterminal Conductance of a Floquet Topological Insulator. *Phys. Rev. Lett.* **2014**, *113*, 266801. [[CrossRef](#)] [[PubMed](#)]
14. Mikami, T.; Kitamura, S.; Yasuda, K.; Tsuji, N.; Oka, T.; Aoki, H. Brillouin-Wigner theory for high-frequency expansion in periodically driven systems: Application to Floquet topological insulators. *Phys. Rev. B* **2016**, *93*, 144307. [[CrossRef](#)]
15. Nagasawa, F.; Frustaglia, D.; Saarikoski, H.; Richter, K.; Nitta, J. Control of the spin geometric phase in semiconductor quantum rings. *Nat. Commun.* **2013**, *4*, 2526. [[CrossRef](#)]
16. Molnár, B.; Peeters, F.M.; Vasilopoulos, P. Spin-dependent magnetotransport through a ring due to spin-orbit interaction. *Phys. Rev. B* **2004**, *69*, 155335. [[CrossRef](#)]
17. Frustaglia, D.; Richter, K. Spin interference effects in ring conductors subject to Rashba coupling. *Phys. Rev. B* **2004**, *69*, 235310. [[CrossRef](#)]
18. Citro, R.; Romeo, F.; Marinaro, M. Zero-conductance resonances and spin filtering effects in ring conductors subject to Rashba coupling. *Phys. Rev. B* **2006**, *74*, 115329. [[CrossRef](#)]
19. Kozin, V.K.; Iorsh, I.V.; Kibis, O.V.; Shelykh, I.A. Quantum ring with the Rashba spin-orbit interaction in the regime of strong light-matter coupling. *Phys. Rev. B* **2018**, *97*, 155434. [[CrossRef](#)]
20. Frustaglia, D.; Nitta, J. Geometric spin phases in Aharonov-Casher interference. *Sol. State Comm.* **2020**, *311*, 113864. [[CrossRef](#)]
21. Meijer, F.E.; Morpurgo, A.F.; Klapwijk, T.M. One-dimensional ring in the presence of Rashba spin-orbit interaction: Derivation of the correct Hamiltonian. *Phys. Rev. B* **2002**, *66*, 033107. [[CrossRef](#)]
22. Eckardt, A.; Anisimovas, E. High-frequency approximation for periodically driven quantum systems from a Floquet-space perspective. *New J. Phys.* **2015**, *17*, 093039. [[CrossRef](#)]
23. Heiss, W.D.; Nazmitdinov, R.G. Orbital magnetism in small quantum dots with closed shells. *JETP Lett.* **1998**, *68*, 915. [[CrossRef](#)]
24. Ihn, T. *Semiconductor Nanostructures*; Oxford University Press: New York, NY, USA, 2010.